Cloud condensation nuclei in pristine tropical rainforest air of Amazonia: size-resolved measurements and modeling of atmospheric aerosol composition and CCN activity

S. S. Gunthe[1], S. M. King[2], D. Rose[1], Q. Chen[2], P. Roldin[3], D. K. Farmer[4], J. L. Jimenez[4], P. Artaxo[5], M. O. Andreae[1], S. T. Martin[2], and U. Pöschl[1]

(1) Max Planck Institute for Chemistry, Biogeochemistry Department, Mainz, Germany

(2) Harvard University, School of Engineering and Applied Sciences & Department of Earth and Planetary Sciences, Cambridge, MA, USA

(3) Lund University, Nuclear Physics, Faculty of Technology, Lund, Sweden

(4) University of Colorado, Dept. of Chemistry & Biochemistry and CIRES, Boulder, CO, USA

(5) Instituto de Fisica, Universidade de Sao Paulo, Sao Paulo, Brazil

Correspondence to: S. Gunthe (gunthe@mpch-mainz.mpg.de)

Online Supplementary Material

Version/Date: 6 August 2009

Table S1: Characteristic CCN parameters (median values) averaged over the entire campaign (14 Feb – 12 Mar 2008), over the pristine focus period (6-12 Mar, 22:00 UTC), and over the rest of the campaign (14 Feb – 6 Mar): midpoint activation diameters (D_a, D_t), maximum activated fractions (MAF_f, MAF_m), heterogeneity parameters (σ_a/D_a, σ_t/D_t), hygroscopicity parameters (κ_a, κ_t), number concentrations of aerosol particles with $D > 30$ nm ($N_{CN,30}$), number concentrations of cloud condensation nuclei ($N_{CCN,s}$), integral CCN efficiencies ($N_{CCN,s}/N_{CN,30}$), number of data points (n). Subscripts a and t stand for parameters derived from 3-parameter and 2-parameter CDF fits to the measured CCN efficiency spectra, respectively. Concentration values are normalized to a reference state of 273 K and 1000 hPa.

S [%]	D_a [nm]	D_t [nm]	MAF_f	MAF_m	σ_a [nm]	σ_t [nm]	σ_a/D_a	σ_t/D_t	κ_a	κ_t	$N_{CN,30}$ [cm^{-3}]	$N_{CCN,S}$ [cm^{-3}]	$N_{CCN,S}/N_{CN,30}$	n
Entire campaign														
0.10	197.9	200.7	0.92	0.93	8.87	13.02	0.04	0.07	0.196	0.187	206	36	0.13	132
0.19	129.1	130.7	0.98	0.98	9.26	10.95	0.07	0.08	0.184	0.177	200	81	0.36	158
0.28	105.5	105.8	1.00	1.00	7.42	7.29	0.07	0.07	0.154	0.153	194	103	0.43	155
0.46	82.6	83.2	1.01	1.01	6.93	7.28	0.09	0.09	0.114	0.112	199	121	0.52	151
0.82	54.4	55.0	1.00	1.00	3.55	3.98	0.07	0.07	0.120	0.119	191	163	0.77	155
All							0.07	0.08	0.149	0.147	204			751
Focus period														
0.10	220.7	224.1	0.88	0.90	7.88	8.92	0.04	0.04	0.143	0.137	217	14	0.06	38
0.19	134.9	135.4	0.99	0.99	6.53	6.33	0.05	0.05	0.164	0.161	215	67	0.32	44
0.28	106.4	106.6	0.99	0.99	5.97	6.21	0.06	0.06	0.150	0.148	217	102	0.39	41
0.46	85.2	86.6	1.01	1.01	5.53	6.38	0.06	0.07	0.105	0.100	216	125	0.50	42
0.82	55.4	55.8	1.01	1.03	2.20	2.10	0.04	0.04	0.118	0.115	202	205	0.78	43
All							0.06	0.06	0.136	0.134	216			208
Rest of campaign														
0.10	190.9	192.4	0.92	0.93	9.88	14.39	0.05	0.07	0.215	0.208	206	43	0.18	94
0.19	126.3	128.1	0.98	0.98	11.22	11.82	0.09	0.09	0.193	0.187	196	85	0.37	114
0.28	104.2	104.1	1.00	1.00	8.31	7.86	0.08	0.08	0.161	0.160	193	103	0.45	114
0.46	81.5	82.1	1.00	1.01	7.71	7.57	0.09	0.10	0.117	0.117	195	119	0.54	109
0.82	54.7	54.9	0.99	1.00	4.59	4.97	0.08	0.09	0.122	0.122	185	152	0.75	112
All							0.09	0.09	0.158	0.154	195			543

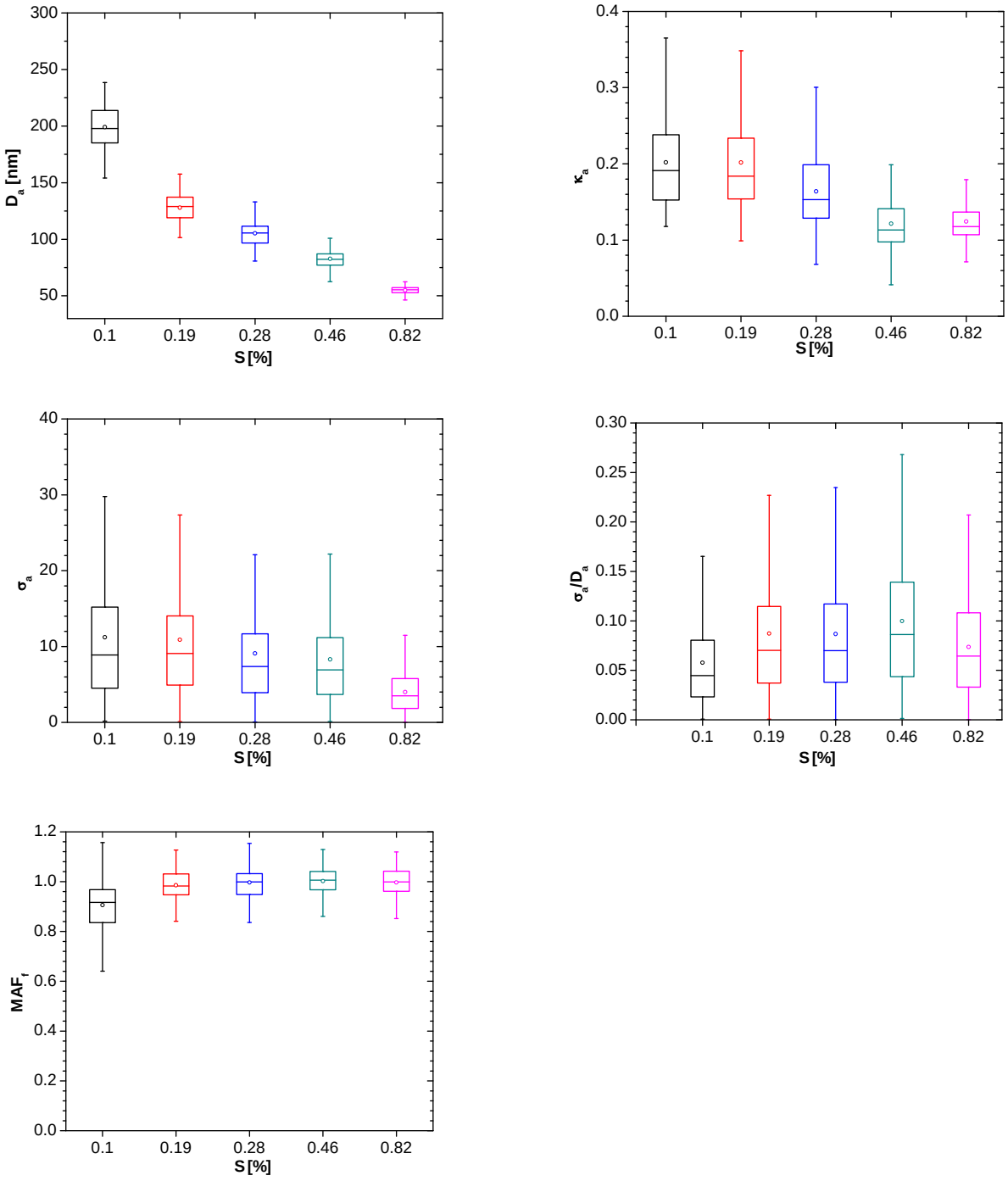

Fig. S1: Statistical distribution of characteristic parameters derived from the CCN efficiency spectra (3-parameter CDF fits) observed at different supersaturations over the entire campaign. Boxes and bars indicate 5th, 25th, 50th, 75th, and 95th percentiles; dots indicate arithmetic mean values.

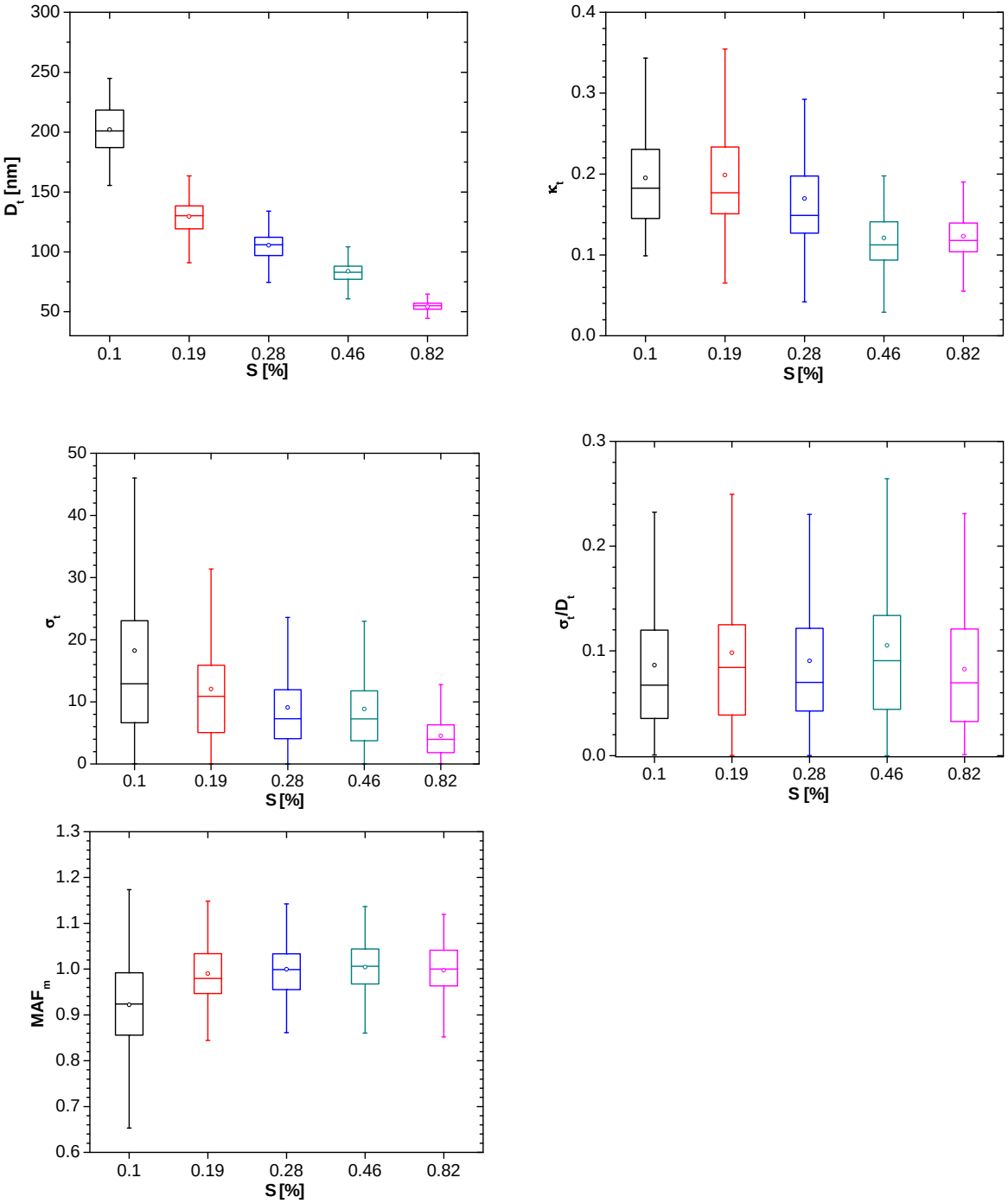

Fig. S2: Statistical distribution of characteristic parameters derived from the CCN efficiency spectra (2-parameter CDF fits) observed at different supersaturations over the entire campaign. Boxes and bars indicate 5th, 25th, 50th, 75th, and 95th percentiles; dots indicate arithmetic mean values.

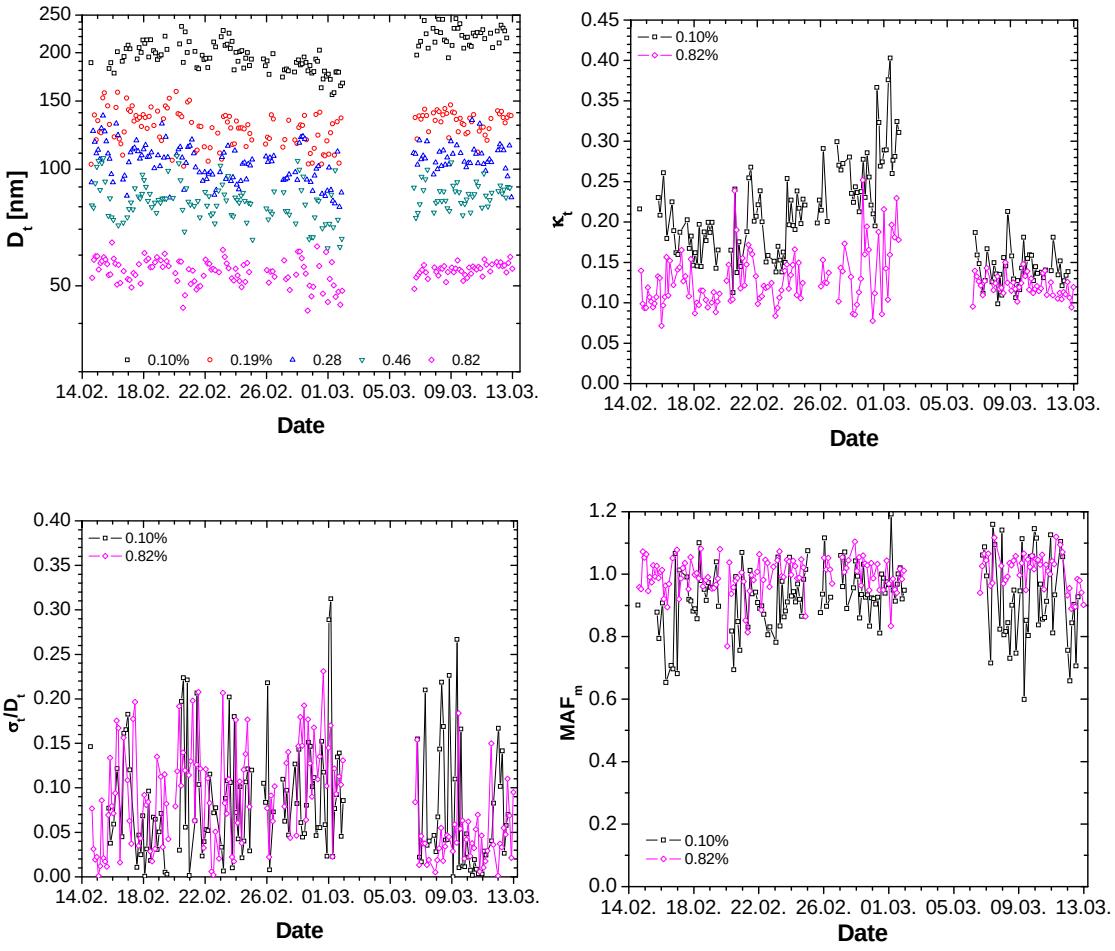

Fig. S3: Time series of characteristic parameters derived from the CCN efficiency spectra (2-parameter CDF fits) observed at different supersaturation levels (S=0.10-0.82%) plotted against the date in Feb-Mar 2008 (UTC): midpoint activation diameter (D_t), effective hygroscopicity diameter (κ_t), heterogeneity parameter (σ_t/D_t), and measured maximum activated fraction (MAF_m).

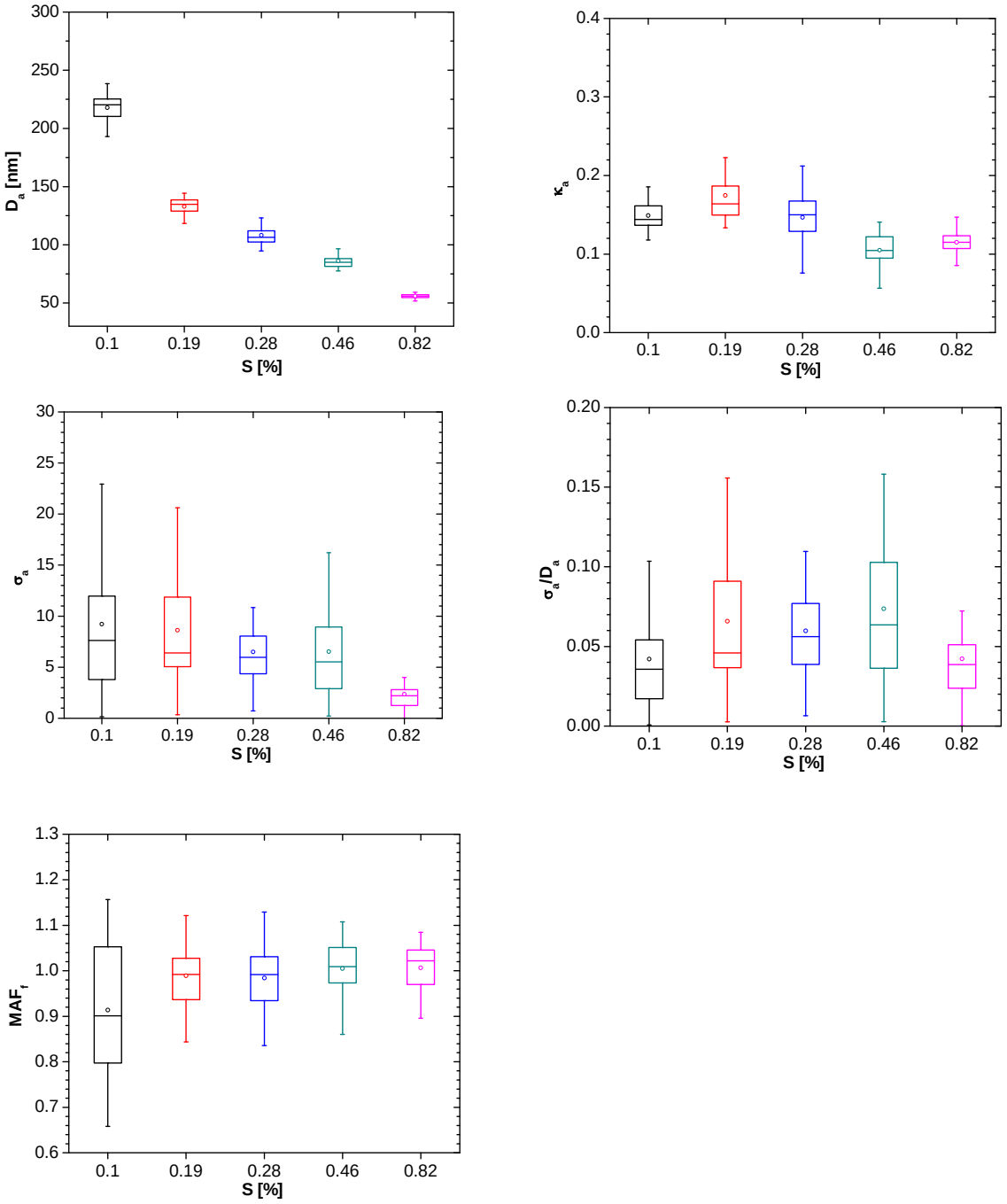

Fig. S4: Statistical distribution of characteristic parameters derived from the CCN efficiency spectra (3-parameter CDF fits) observed at different supersaturations during the focus period, 6-12 March 2008. Boxes and bars indicate 5th, 25th, 50th, 75th, and 95th percentiles; dots indicate arithmetic mean values.

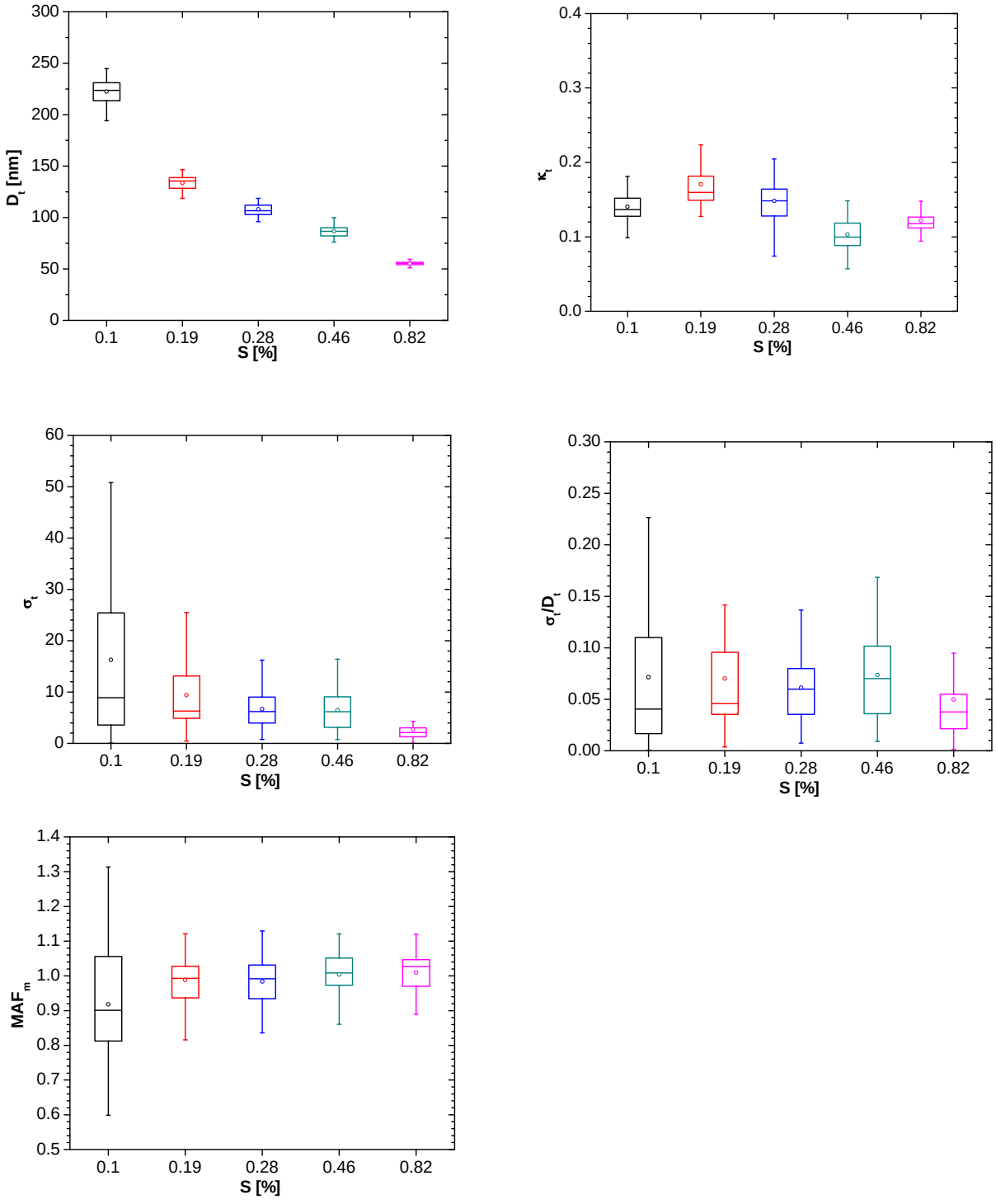

Fig. S5: Statistical distribution of characteristic parameters derived from the CCN efficiency spectra (2-parameter CDF fits) observed at different supersaturation levels during the focus period, 6-12 March 2008. Boxes and bars indicate 5th, 25th, 50th, 75th, and 95th percentiles; dots indicate arithmetic mean values.

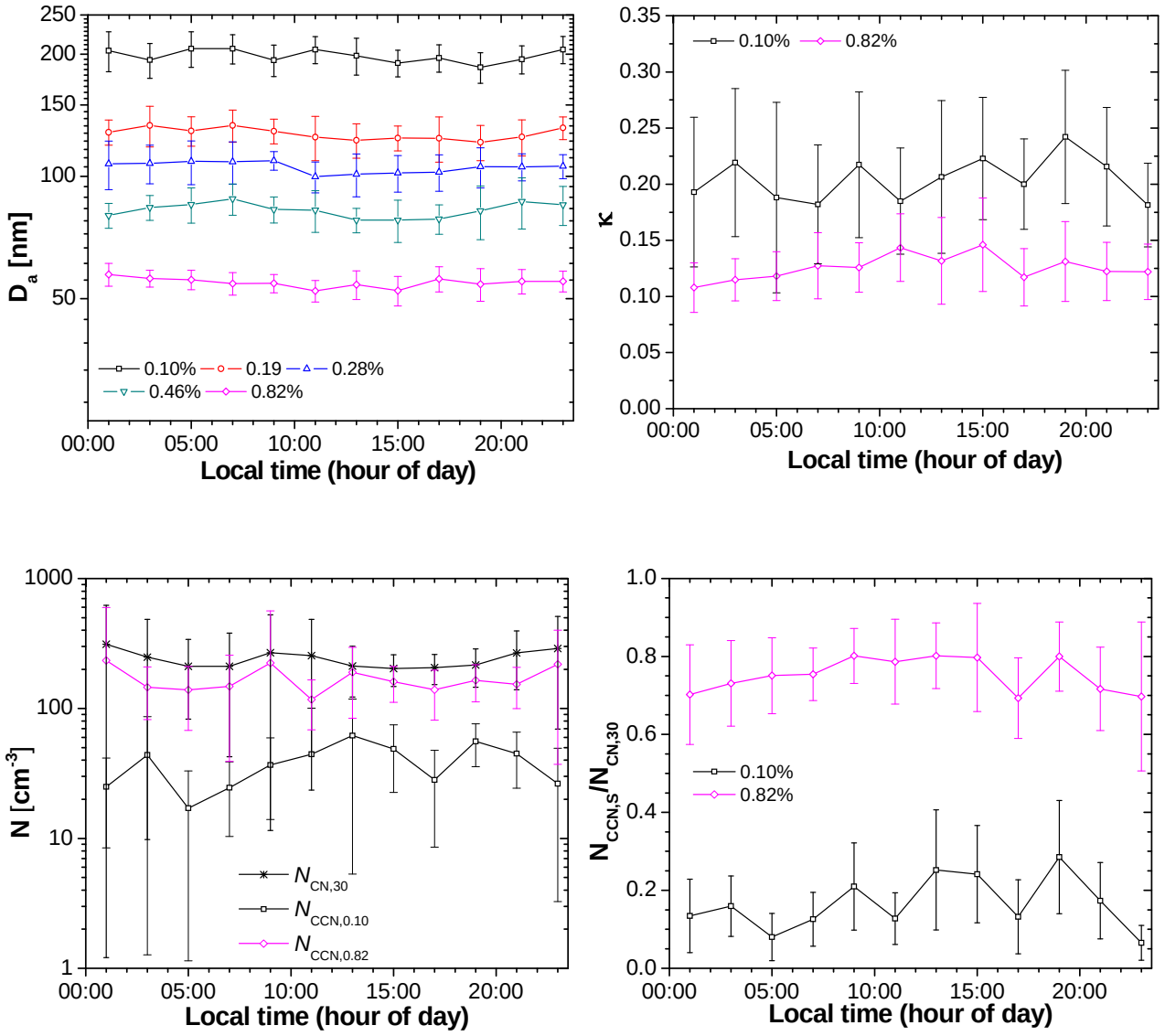

Fig. S6: Diel variation of midpoint activation diameter (D_a), hygroscopicity parameter (κ_a), number concentrations of aerosol particles with D >30 nm ($N_{CN,30}$) and cloud condensation nuclei ($N_{CCN,S}$), and integral CCN efficiencies ($N_{CCN,S}/N_{CN,30}$) for different supersaturation levels averaged of the entire campaign (two-hour intervals). Data points and error bars represent arithmetic mean ± standard deviation.

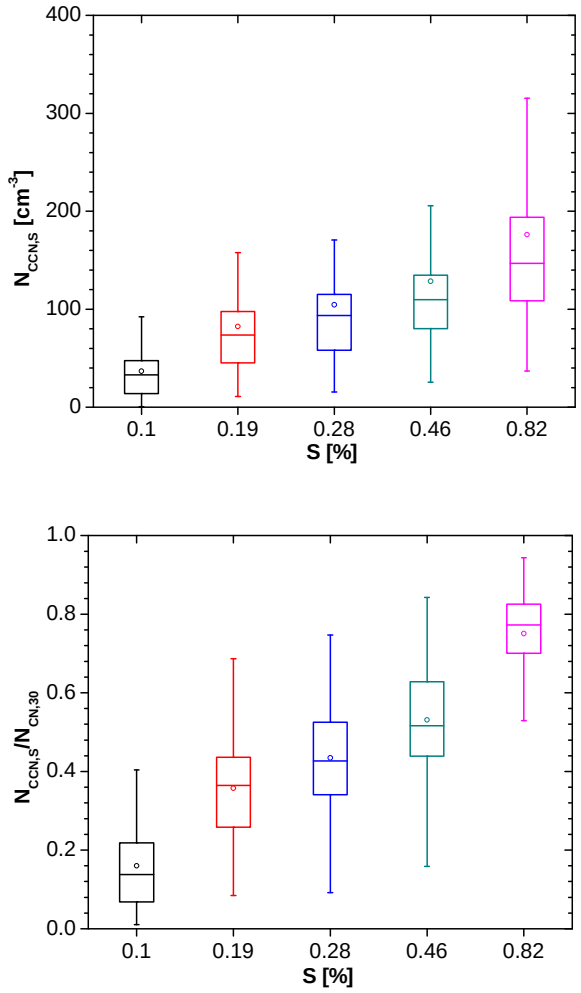

Fig. S7: Statistical distribution of CCN number concentrations ($N_{CCN,S}$) and integral CCN efficiencies ($N_{CCN,S}/N_{CN,30}$) observed at different supersaturations over the entire campaign. Boxes and bars indicate 5th, 25th, 50th, 75th, and 95th percentiles; dots indicate arithmetic mean values.

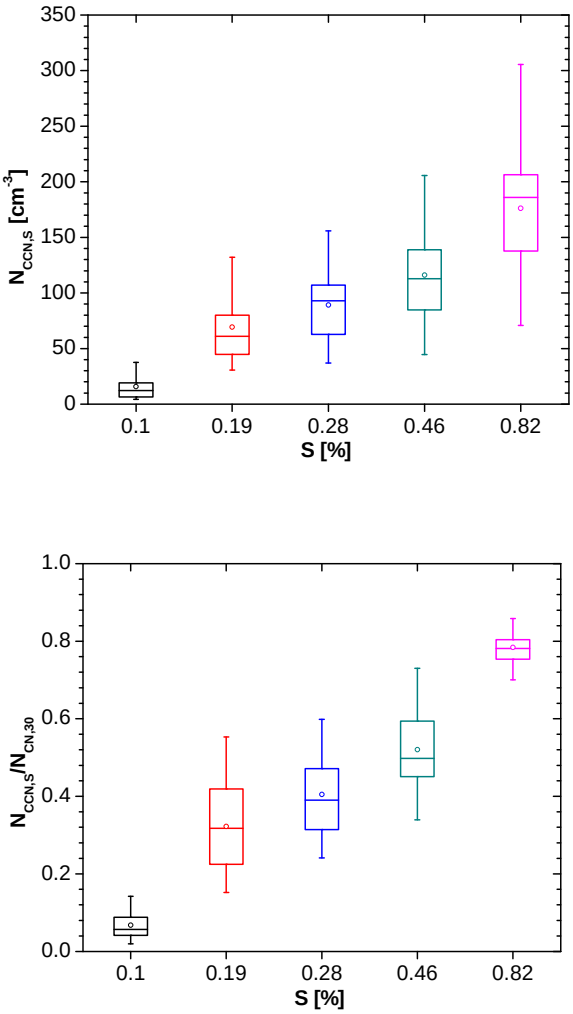

Fig. S8: Statistical distribution of CCN number concentrations ($N_{CCN,S}$) and integral CCN efficiencies ($N_{CCN,S}/N_{CN,30}$) observed at different supersaturations during the focus period, 6-12 March 2008. Boxes and bars indicate 5th, 25th, 50th, 75th, and 95th percentiles; dots indicate arithmetic mean values.

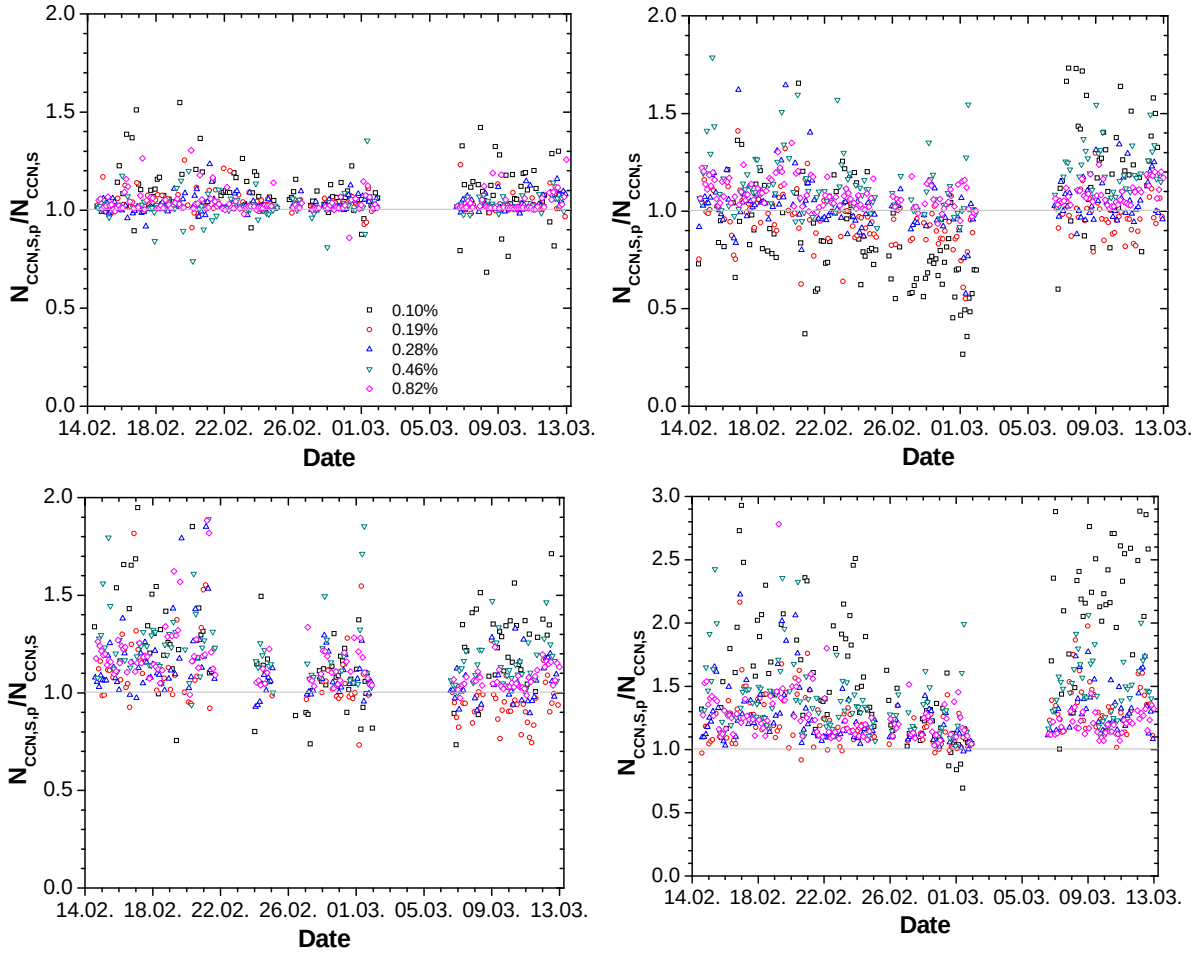

Fig. S9: Time series of the ratio of predicted and measured CCN concentrations ($N_{CCN,S,p}/N_{CCN,S}$) plotted against the date in Feb-Mar 2008 (UTC). Predictions are based on the κ-Köhler model approach using different types of effective hygroscopicity parameters: (a) variable values of κ_t as derived from the individual CCN efficiency spectra; (b) constant campaign median value $\kappa = 0.15$; (c) variable values of κ_p predicted with organic and inorganic mass fractions determined by integral AMS measurements; and (d) constant approximate global average value $\kappa = 0.3$.

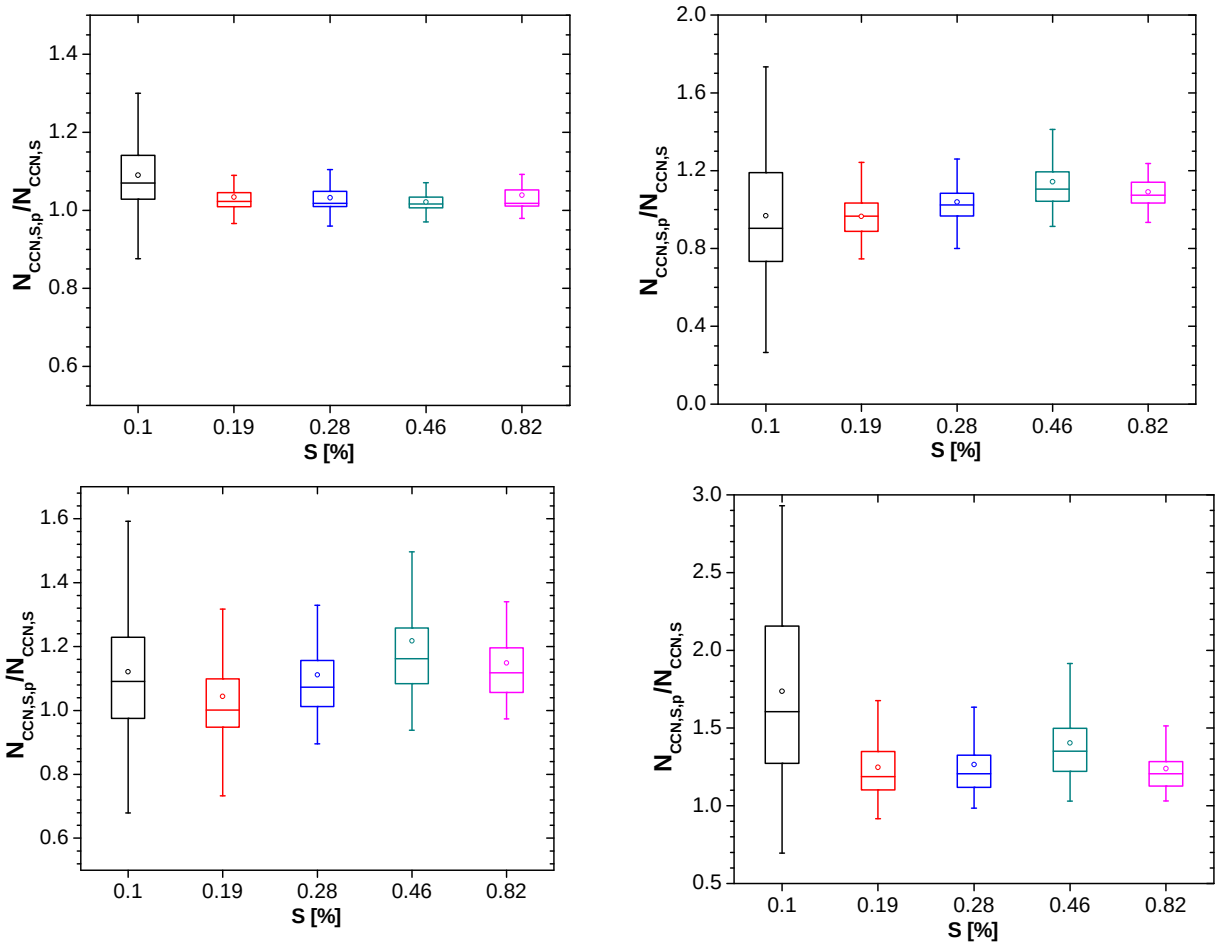

Fig. S10: Statistical distribution of the ratios of predicted and measured CCN concentrations ($N_{CCN,S,p}/N_{CCN,S}$) at different supersaturation level over the entire campaign. Predictions are based on the κ-Köhler model approach using different types of effective hygroscopicity parameters: (a) variable values of κ_t as derived from the individual CCN efficiency spectra; (b) constant campaign median value $\kappa = 0.15$; (c) variable values of κ_p predicted with organic and inorganic mass fractions determined by AMS; and (d) constant approximate global average value $\kappa = 0.3$. Boxes and bars indicate 5th, 25th, 50th, 75th, and 95th percentiles; dots indicate arithmetic mean values.